JOURNAL OF VIROLOGY, Oct. 2009, p. 10176–10186 Vol. 83, No. 19
0022-538X/09/$08.00+0 doi:10.1128/JVI.00422-09

Rho GTPases Modulate Entry of Ebola Virus and Vesicular Stomatitis Virus Pseudotyped Vectors▽

Kathrina Quinn,[1] Melinda A. Brindley,[2] Melodie L. Weller,[1] Nikola Kaludov,[1] Andrew Kondratowicz,[2] Catherine L. Hunt,[2] Patrick L. Sinn,[3] Paul B. McCray, Jr.,[2,3] Colleen S. Stein,[4] Beverly L. Davidson,[4,5,6] Ramon Flick,[7] Robert Mandell,[7] William Staplin,[7] Wendy Maury,[2] and John A. Chiorini[1]*

Molecular Physiology and Therapeutics Branch, National Institute of Dental and Craniofacial Research, National Institutes of Health, Bethesda, Maryland 20892[1]; Department of Microbiology[2] and Department of Pediatrics,[3] Carver College of Medicine, University of Iowa, Iowa City, Iowa 52242; Department of Internal Medicine,[4] Department of Neurology,[5] and Department of Physiology and Biophysics,[6] University of Iowa College of Medicine, Iowa City, Iowa 52242; and BioProtection Systems, Ames, Iowa 50011[7]

Received 26 February 2009/Accepted 15 July 2009

To explore mechanisms of entry for Ebola virus (EBOV) glycoprotein (GP) pseudotyped virions, we used comparative gene analysis to identify genes whose expression correlated with viral transduction. Candidate genes were identified by using EBOV GP pseudotyped virions to transduce human tumor cell lines that had previously been characterized by cDNA microarray. Transduction profiles for each of these cell lines were generated, and a significant positive correlation was observed between RhoC expression and permissivity for EBOV vector transduction. This correlation was not specific for EBOV vector alone as RhoC also correlated highly with transduction of vesicular stomatitis virus GP (VSVG) pseudotyped vector. Levels of RhoC protein in EBOV and VSV permissive and nonpermissive cells were consistent with the cDNA gene array findings. Additionally, vector transduction was elevated in cells that expressed high levels of endogenous RhoC but not RhoA. RhoB and RhoC overexpression significantly increased EBOV GP and VSVG pseudotyped vector transduction but had minimal effect on human immunodeficiency virus (HIV) GP pseudotyped HIV or adeno-associated virus 2 vector entry, indicating that not all virus uptake was enhanced by expression of these molecules. RhoB and RhoC overexpression also significantly enhanced VSV infection. Similarly, overexpression of RhoC led to a significant increase in fusion of EBOV virus-like particles. Finally, ectopic expression of RhoC resulted in increased nonspecific endocytosis of fluorescent dextran and in formation of increased actin stress fibers compared to RhoA-transfected cells, suggesting that RhoC is enhancing macropinocytosis. In total, our studies implicate RhoB and RhoC in enhanced productive entry of some pseudovirions and suggest the involvement of actin-mediated macropinocytosis as a mechanism of uptake of EBOV GP and VSVG pseudotyped viral particles.

Enveloped viruses enter cells by a variety of different pathways. Productive internalization of enveloped viruses with targeted cells is mediated through interactions of the viral glycoprotein(s) (GPs) with moieties on the surface of the cell. In general, enveloped viral entry occurs through viral adherence to the cell surface, interaction with a specific plasma membrane-associated receptor that results in a series of GP conformational changes leading to fusion of viral and cellular membranes, and delivery of the viral core particle into the cytoplasm. Fusion of the two membranes can occur at the plasma membrane or by uptake of the intact virions into endosomes with subsequent membrane fusion between the viral membrane and the lipid bilayer of the endocytic vesicle. Human immunodeficiency virus (HIV) is an example of a virus that fuses directly to the plasma membrane (5), whereas influenza virus must be internalized into acidified vesicles where the appropriate GP conformational changes can occur, mediating membrane fusion (21). Most enveloped viruses that enter through vesicles utilize a low-pH environment to mediate the necessary conformational changes in GP that induce membrane fusion (37).

Ebola virus (EBOV) and vesicular stomatitis virus (VSV) are enveloped, single-stranded, negative-sense RNA viruses belonging to the families *Filoviridae* and *Rhabdoviridae*, respectively. Though they share similarity in genome organization and a broad tropism for a variety of cell types, they differ greatly in their pathogenicities (29, 39). EBOV causes severe hemorrhagic fever that is frequently fatal, whereas VSV infects mainly livestock, generating fluid-filled vesicles on mucosal surfaces.

Interestingly, the receptor(s) that mediate entry of these two viruses have yet to be definitively identified. C-type lectins such as DC-SIGN and DC-SIGNR are thought to serve as adherence factors for EBOV (26). Other plasma membrane-associated proteins have been implicated in EBOV uptake including folate receptor alpha and the tyrosine kinase receptor Axl (6, 35, 36, 38), but the physical interaction of EBOV GP and these proteins has not been demonstrated, and cells that do not express these proteins are permissive for EBOV GP-mediated virion uptake. VSV was shown to bind ubiquitously to cells via phosphatidylserine (PS) (31). However, a more recent study

* Corresponding author. Mailing address: Molecular Physiology and Therapeutics Branch, National Institute of Dental and Craniofacial Research, National Institutes of Health, Building 10, Room 1421, Bethesda, MD 20892. Phone: (301) 496-4279. Fax: (301) 402-1228. E-mail: Jchiorini@dir.nidcr.nih.gov.

▽ Published ahead of print on 22 July 2009.

reports that PS is not a receptor for VSV as no correlation was found between cell surface PS levels and VSV infection, and annexin V, which binds specifically to PS, did not inhibit infection of VSV (9).

Both viruses enter cells through a low-pH-dependent, endocytosis-mediated process. A large body of evidence indicates that VSV is internalized via clathrin-coated pits, with a reduction in pH mediating reversible alterations in the GP leading to membrane fusion (40). EBOV may also enter cells by clathrin-mediated endocytosis (30), but lipid raft-associated, caveolin-mediated endocytosis has also been proposed as a mechanism of EBOV uptake (11). Low-pH events lead to cathepsin-dependent cleavage of EBOV GP that is required for productive uptake of the virus (8, 19, 33). Other low-pH-dependent events have been postulated to be required as well (33).

To identify genes whose expression correlated with EBOV GP-dependent transduction, we compared the relative transduction efficiency of EBOV GP pseudotyped virions on a panel of human tumor cell lines with gene expression data from cDNA microarrays developed for the same panel of cell lines (20). The gene array data are available from the Developmental Therapeutics Program at the National Cancer Institute (NCI) website (http://dtp.nci.nih.gov/). A significant correlation was observed between expression of RhoC, a member of the small GTP-binding Rho GTPase family, and permissivity for EBOV transduction. Surprisingly, a significant correlation was also observed between VSV glycoprotein (VSVG)-mediated transduction and RhoC expression. In this study, we report that modulation of RhoC expression by transfection of expression plasmids or treatment with an inhibitor alters transduction by virions pseudotyped with either EBOV GP or VSVG and fusion of EBOV virus-like particles (VLPs). RhoC expression also significantly enhanced wild-type VSV infection. We also examine the differential effect each Rho GTPase has on nonspecific endocytotic uptake of exogenous material and on organization of the actin filament. Our findings suggest that RhoC enhances entry of EBOV GP and VSVG pseudovirions through modulation of fluid-phase endocytosis.

MATERIALS AND METHODS

Cell lines. For transduction studies, human embryonic kidney (HEK) 293T cells, African green monkey Cos-7 cells, Vero cells, producer 2E6 cells, and human glioblastoma SNB-19 cells (http://dtp.nci.nih.gov/branches/btb/tumor-catalog.pdf) were all grown in high-glucose Dulbecco's modified Eagle's medium (DMEM) supplemented with 10% (vol/vol) fetal bovine serum (FBS), 1% (vol/vol) penicillin and streptomycin (Pen-Strep), and 1% (vol/vol) L-glutamine (Gibco). Human Malme-3M cells (http://dtp.nci.nih.gov/branches/btb/tumor-catalog.pdf) were maintained in RPMI medium supplemented with 10% (vol/vol) FBS and 1% (vol/vol) Pen-Strep. All NCI60 lines used in the comparative genomic analysis screens (http://dtp.nci.nih.gov/branches/btb/tumor-catalog.pdf) were grown in RPMI medium supplemented with 5% (vol/vol) FBS and 1% (vol/vol) Pen-Strept.

Plasmids. Expression plasmids for human RhoA, RhoB, and RhoC were obtained from Origene. Control expression plasmid pCMV-script came from Stratagene. A Src-β-lactamase-expressing plasmid was constructed by first cloning the coding region of the β-lactamase gene (270 amino acids; from pBluescript) into pCMV-script vector using HindIII and SalI sites, followed by the first N-terminal 15 amino acids of c-Src tyrosine kinase into PstI and HindIII using polylinkers. A polyglutamine region was included downstream of the c-Src region. Primers and polylinkers were as follows: forward β-lactamase primer, 5′-GGCGTCGACTTACCAATGCTTAATCAGTGA-3′; reverse β-lactamase primer, 5′-GGAAAGCTTATGCTTCCTGTTTTTGCTCA-3′; forward c-Src polylinker, 3′-GCATGGGGAGCAGCAAGAGCAAGCCCAAGGACCCCAGCCAGCGCCGGAACAACAACGGGA-3′; reverse c-Src polylinker, 5′-AGCTTCCCGTTGTTGTTCCGGCGCTGGCTGGGGTCCTTGGGCTTGCTCTTGCTGCTCCCCATGCTGCA-3′. Plasmids expressing adeno-associated virus 2 encoding luciferase (AAV2-luciferase) and AAV2-nuclear green fluorescent protein (GFP) were supplied within the laboratory. All plasmids used to generate feline immunodeficiency virus (FIV) and VSV core pseudovirions have been previously described (3, 42). All plasmids used to generate HIV and murine leukemia virus (MuLV) core pseudovirions are commercially available from Invitrogen and Clontech, respectively. EBOV nucleocapsid protein (NP) and VP40 plasmids were kindly provided by R. Harty (Department of Pathobiology, School of Veterinary Medicine, University of Pennsylvania) and have been previously described (15).

Antibodies and reagents. Rabbit polyclonal anti-Src antibody and mouse monoclonal anti-human RhoA, RhoB, and RhoC antibodies were purchased from Abcam. A CCF2/AM loading kit, Alexa Fluor 488-dextran conjugate, and Alexa Fluor 546-phallotoxin probe came from Invitrogen. Benzonase and protease cocktail inhibitor were from Sigma. *Clostridium difficile* toxin B was purchased from Calbiochem. CellTiter 96 Aqueous One Solution proliferation reagent was from Promega. The ATP Lite cell viability kit was from the Packard Corporation.

Viral particle and VLP production. (i) Production of EBOV GP pseudotyped FIV-β-galactosidase particles (EBOV/FIV-β-galactosidase). FIV virions were generated as previously described (3). Virus was produced by transfection of three plasmids into 80% confluent HEK 293T cells in a total of 75 μg of plasmid DNA. The transfected plasmids consisted of the following at a ratio of 1:2:3, respectively: pCMV/EBOVΔO that expresses EBOV GP with a deletion of the mucin domain, pCMV/FIVΔΔ that expresses FIV *gag-pol*, and pFIVψβgal. The DNA was transfected into 15-cm diameter dishes of 293T cells using calcium phosphate transfection (16). After 12 h the cells were washed, and fresh medium was added (DMEM, 2% [vol/vol] FBS, 1% [vol/vol] Pen-Strep). Supernatants were collected at 24, 36, 48, 60, and 72 h posttransfection and frozen at −80°C. The supernatants were thawed, filtered through a 0.45-μm-pore-size filter, and pelleted by a 16-h centrifugation step (7,700 × *g* at 4°C in a Sorvall GSA rotor). The viral pellet was resuspended in DMEM for an approximate 200-fold concentration. A reverse transcriptase (RT) assay was performed, viral input was normalized for RT activity (28), and the virus was either used immediately for infection or stored at −80°C until use.

(ii) Production of VSV/VSV-eGFP and EBOV/VSV-eGFP particles. VSV encoding an enhanced green fluorescent protein (VSV-eGFP) reporter gene was pseudotyped with either the native GP or EBOV GP (VSV/VSV-eGFP or EBOV/VSV-eGFP, respectively) as previously described (42). Briefly, 15-cm diameter plates of 80% confluent 293T cells were transfected with 75 μg of pcDNA3.1 plasmid expressing VSVG or EBOVΔO GP using the calcium phosphate transfection procedure (16). Cells were rinsed with phosphate-buffered saline (PBS) 12 h later to remove the transfection reagents. At 24 h following transfection, cells were transduced with VSVG pseudotyped VSVΔG-eGFP (multiplicity of infection [MOI] of ~0.1). Viral inoculum was removed 12 h later, and supernatants were collected at 24 h following transduction for viral stocks. Stocks were serially diluted on Vero cells, and titers were evaluated by eGFP expression.

(iii) Production of EBOV GP and VSVG pseudotyped MuLV-eGFP particles(EBOV/MuLV-eGFP and VSV/MuLV-eGFP, respectively). Producer 2E6 cells that were derived from 293T cells stably express MuLV Gag/Pol proteins and MuLVψeGFP. 2E6 cells were plated in 15-cm plates and transfected with 75 μg of either pCMV/EBOVΔO or pCMV/VSVG using the calcium phosphate transfection procedure, and supernatant was harvested and concentrated as described above. Particle titrations were performed on SNB-19 cells.

(iv) Production of EBOV GP and HIV pseudotyped HIV-eGFP particles (EBOV/HIV-eGFP and HIV/HIV-eGFP, respectively). Protocols to generate HIV-based particles were similar to the FIV-based virion production described above except that the transfection was composed of a four-plasmid system that included the following at a ratio of 1:2:1:3, respectively: pCMV/EBOVΔO or p962M651gp160 that expresses a codon-optimized HIV gp160, pCMV/HIV *gag-pol*, pCMV/Rev, and pHIVψeGFP. Particle titrations were performed on SNB-19 cells.

(v) Production of EBOV GP pseudotyped VLPs. Src-β-lactamase-labeled EBOV VLPs were produced as follows: 293T cells were grown in six 15-cm dishes to 75% confluence and transfected with 75 μg of total DNA at a ratio of 1:2:3:3 for plasmids expressing EBOV NP, EBOV VP40, EBOV GP, and Src-β-lactamase (prepared as described above) using a calcium phosphate transfection procedure (16). EBOV GP-deficient VLPs were prepared by transfecting 293T cells with 75 μg of total DNA at a ratio of 1:2:3:3 for plasmids expressing EBOV NP, EBOV VP40, empty pcDNA prep, and Src-β-lactamase. Supernatants were collected at 24, 36, 48, 60, and 72 h following transfection. The

supernatants were filtered through a 0.45-μm-pore-size filter and pelleted by an overnight centrifugation step (5,400 × *g* at 4°C in a Beckman JA-10 rotor). The viral pellet was resuspended in DMEM for an approximate 200-fold concentration. The virus was stored at −80°C until use. Incorporation of Src-β-lactamase (approximately 32 kDa) was detected by immunoblotting. Proteins present in 10 μl of concentrated VLPs were separated on a 12% Bis-Tris-polyacrylamide electrophoresis gel and transferred to a nitrocellulose membrane. The membrane was blocked overnight with 10% (vol/vol) milk in PBS–0.05% Tween 20 (PBS-T) and incubated with rabbit polyclonal anti-Src primary antibody (1:1,000) in 2% (vol/vol) milk in PBS-T for 2 h at room temperature, followed by horseradish peroxidase-conjugated anti-rabbit secondary antibody (1:20,000) in 10% (vol/vol) milk in PBS-T for 1 h at room temperature. The bands were visualized with Supersignal West Dura substrate (Pierce).

Comparative genomic analysis studies. Forty-six cell lines from the National Cancer Institute 60-cell-line cancer panel (NCI60) were maintained as previously described (20), and their relative transduction efficiencies were determined by transduction with EBOV/FIV-β-galactosidase in an end point serial dilution. At 72 h after transduction, the cells were fixed in 3.7% formalin and stained with X-Gal (5-bromo-4-chloro-3-indolyl-D-galactopyranoside) for β-galactosidase activity. Biological titers were determined by counting β-galactosidase-positive cells in the limiting dilution. For comparison with the gene expression array data, the average of the relative transduction efficiencies for all the cells was then determined, and a log transformation of the deviation from the average for each cell type was used to generate a profile. This file was then used as seed data for an established analysis called COMPARE (48). COMPARE ranks an entire database of cDNA expression arrays in order of similarity of responses of the 60 cell lines to the compounds in the database to the responses of the cell lines to the seed compound. Similarity of pattern to that of the seed is expressed quantitatively as a Pearson correlation coefficient (PCC). COMPARE analysis was repeated using transduction data generated from EBOV/VSV-eGFP and VSV/VSV-eGFP vectors as seed. Fifty-four of the NCI 60 cell lines were transduced with equal amounts of pseudotyped vector. Relative transduction efficiencies were determined by analyzing eGFP positivity via flow cytometry 24 h later. All trials were performed three independent times. Data were analyzed by Win MDI software to determine the percentage of the cell population expressing eGFP.

Transduction of permissive and weakly permissive cells with EBOV/MuLV-eGFP or VSV/MuLV-eGFP vectors. HEK 293T, Cos-7, SNB-19, and Malme-3M cells were seeded in triplicate at 3×10^4 cells per well of 96-well plate for 24 h. Cells were transduced with either EBOV/MuLV-eGFP or VSV/MuLV-eGFP particles at an MOI of 1.5 for 60 h. Transduction efficiencies were determined by quantifying the percentage of eGFP-expressing cells using a custom BD fluorescence-activated cell sorter (FACSArray) fitted with a blue laser and 530/bp30 filter. Data were analyzed by FlowJo, version 7.2, software to determine the percentage of the cell population expressing eGFP. The experiment was performed three times. Mean percentage transduction was calculated for both vectors.

Western blot analysis for Rho GTPases. HEK 293T, Cos-7, SNB-19, and Malme-3M cells were seeded at 3×10^5 cells per well of a six-well plate. After 24 h cells were lysed with 2% sodium dodecyl sulfate containing 0.25 U of benzonase (Sigma) and a 1:100 dilution of protease cocktail inhibitors (Sigma) (250 μl per well). Cell lysate was centrifuged at 10,000 × *g* for 2 min to remove cell debris, aliquoted, and stored at −20°C. A total of 50 μg/lane of cell lysate was run on a 12% Bis-Tris gel (Invitrogen) and transferred semidry onto nitrocellulose membrane for 1 h at 15 V. The membrane was blocked for 30 min in 5% (vol/vol) milk in Tris-buffered saline–0.05% Tween 20 (TBST) and then incubated with either of the following primary antibodies: mouse anti-RhoA, anti-RhoB, or anti-RhoC (1:100 dilution as per the manufacturer's protocol) in 5% (vol/vol) milk in TBST, followed by incubation with anti-mouse secondary antibody (1:5,000 dilution; Amersham) in 5% (vol/vol) milk in TBST. All washes were carried out in TBST. The bands were visualized using ECL chemiluminescent substrate reagent (Amersham). In order to detect the expression of RhoC in 293T cells, more cell lysate was loaded than with the other cell types tested. Band intensity was quantified using Adobe Photoshop CS2 software. Relative intensity was determined by normalizing to glyceraldehyde-3-phosphate dehydrogenase (GAPDH) by dividing the absolute intensity for each sample band by absolute intensity of the GAPDH control band.

Cotransfection with Rho GTPase and luciferase-expressing plasmids followed by transduction with EBOV/MuLV-eGFP or VSV/MuLV-eGFP, EBOV/HIV-eGFP or HIV/HIV-eGFP, and AAV2-GFP. A total of 4×10^4 HEK 293T cells were transiently cotransfected with 0.2 μg of either RhoA, RhoB, or RhoC plasmids together with 0.02 μg of AAV2-luciferase plasmid per well of a 96-well plate using Effectene transfection reagent (Qiagen). pCMV-script plasmid and AAV2-luciferase plasmid were cotransfected as a negative control. All wells were done in triplicate. After 24 h, the cells were transduced with EBOV/MuLV-eGFP, VSV/MuLV-eGFP, EBOV/HIV-eGFP, and HIV/HIV-eGFP at an MOI of 1.5, and percent eGFP expression was measured after 60 h by FACS. Cells were transduced with AAV2-GFP at an MOI of 2,500, and percent GFP expression was measured after 48 h. Transfection efficiency of the remaining cells was determined by addition of Bright-Glo luciferase substrate (1:5 dilution; Promega) to each well, and the number of relative light units (RLU) was measured with an OptocompII luminometer (MGM instruments). Transduction efficiency was then normalized against luciferase activity by expressing the percentage of GFP cells per 500,000 RLU. The experiment was performed three times. The mean relative increase over the pCMV control was calculated for RhoA-, RhoB-, and RhoC-transfected, transduced cells.

Cotransfection with Rho GTPase and eGFP-expressing plasmids followed by infection with VSV. A total of 5×10^5 293T cells were transfected with 3.2 μg of empty pCMV plasmid, the RhoB-expressing plasmid, or the RhoC-expressing plasmid. All transfections included 0.8 μg of eGFP-expressing plasmid to allow evaluation of transfection efficiency that was assessed at 24 h following transfection. Transfected cells were distributed into 24-well trays the following day. At 48 h following transfection, cells were either left untreated or infected with VSV (Indiana strain) at an MOI of 0.0001. VSV-infected cells were held at room temperature for 10 m following initiation of infection and then shifted to 37°C for the remainder of the infection. Two hours following infection, medium was changed to remove any input virus that was not attached or internalized. Supernatant was collected at 18 h following infection and centrifuged to remove any cellular debris.

Titers of virus stocks produced in the transfected cells were determined on Vero cells. Cells were plated in 48-well trays at a concentration of 4×10^4 cells/well. Serial dilutions of VSV generated in the transfected 293T cells were added to the cells. All infections were performed in replicates of six. At 38 h following initiation of infection, cells were washed twice with PBS to remove any detached or dead cells in the wells, and cell viability of the adherent cells was assessed using an ATP Lite cell viability kit (Packard Corporation) per the manufacturer's instructions.

Treatment of Rho GTPase-expressing cells with *C. difficile* toxin B. A total of 4×10^4 HEK 293T cells were transiently cotransfected with 0.2 μg of either RhoA, RhoB, or RhoC plasmids together with 0.02 μg of AAV2-luciferase plasmid per well of a 96-well plate using Effectene transfection reagent. All wells were done in triplicate. After removal of the transfection mixture, cells were incubated in the presence of 600 ng of *C. difficile* toxin B, a known inhibitor of Rho GTPases, in 100 μl of DMEM for 1 h at 37°C. Untreated, transfected cells were included as controls. After 1 h toxin was removed, and cells were transduced with EBOV/MuLV-eGFP at an MOI of 1.5. After 60 h transduction efficiency was determined by eGFP expression and normalized against 500,000 RLU as before. The experiment was performed three times. Mean percent transduction inhibition was calculated by comparison of *C. difficile* toxin B-treated, transfected cells to untreated, transfected cells.

Imaging of EBOV VLP fusion assay. HEK 293T cells were seeded at 3×10^4 cells per well of a 96-well plate and transfected with 0.2 μg of either RhoA, RhoC, or pCMV-script plasmid for 24 h using Effectene transfection agent. After removal of the transfection mixture, cells were incubated with 50 μl of concentrated Src-β-lactamase-labeled EBOV VLPs (as prepared above) per well at 37°C. Untransfected cells were incubated with 50 μl of EBOV GP-deficient VLPs as a negative control. After 12 h EBOV VLPs were removed, and 0.1 mM CCF2/AM, a substrate for β-lactamase, was added to each well, diluted in 100 μl of DMEM according to the manufacturer's protocol (Invitrogen). The plate was covered and incubated at room temperature for 2 h away from direct sunlight. Cells were visualized by fluorescence microscopy (Nikon Diaphot) using a β-lactamase filter (Chroma 41031) (20× objective). Positive controls for the β-lactamase assay included pCMV-Src-β-lactamase-transfected and blue fluorescent protein-transfected cells. Images were analyzed using ImageJ software. Blue fluorescence was measured in five threshold images and is expressed per square pixel; particles outside the range of the specified size of an average cell were not measured. The background blue fluorescence of untransfected, untreated control cells was subtracted from the fluorescence of transfected, VLP-treated cells. The mean relative increase in blue fluorescence over pCMV-transfected, VLP-treated controls was calculated for RhoA- and RhoC-transfected, VLP-treated cells.

Alexa Fluor 488-fluorescent dextran uptake assay. HEK 293T cells were seeded at 3×10^4 cells per well of a 96-well plate and cotransfected with 0.2 μg of either RhoA, RhoC, or pCMV-script plasmid together with 0.02 μg of AAV2-luciferase plasmid. All wells were done in triplicate. After 24 h, the transfection mixture was removed, and 20 μg of Alexa Fluor 488-dextran conjugate was added to each well, diluted in 100 μl of DMEM. After a 40-min incubation at

37°C, the percentage of dextran uptake was measured using a custom BD fluorescence-activated cell sorter (FACSArray) fitted with a blue laser and 530/bp30 filter. Transfection efficiency of the remaining cells was determined, and overall dextran uptake was expressed as a percentage of Alexa Fluor 488-positive cells per 500,000 RLU. The experiment was performed three times. The mean relative increase over the pCMV control was calculated for RhoA- and RhoC-transfected cells.

Immunofluorescence to visualize actin reorganization by Rho GTPases. Cos-7 cells were seeded in glass-bottomed microwell dishes at 3×10^5 cells per dish. After 24 h cells were cotransfected with either 0.4 μg of RhoA, RhoC, or pCMV-script control plasmid together with 0.04 μg of AAV2-nuclear GFP plasmid. Untransfected cells were included as a negative control. After 24 h, F-actin was labeled with Alexa Fluor 546-conjugated phallotoxin probe (Invitrogen/Molecule Probes). Cells were fixed with 2% paraformaldehyde for 15 min at room temperature and then permeabilized with 0.1% Triton X-100 for 5 min. Cells were blocked with 6% FBS for 30 min at 37°C and incubated with 1 unit of fluorescent phallotoxin per dish for 20 min at room temperature. All washes were carried out in 1× PBS. Hard-set mounting medium (Vector Labs) was added to each dish, and cells were visualized by confocal microscopy (63× oil immersion objective). Successfully transfected cells were identified by nuclear GFP fluorescent staining, and images of eight positive cells were captured and quantified using ImageJ imaging software. Background Alexa Fluor 546 fluorescence of untransfected cells was subtracted, and the mean relative increase in actin fluorescence over pCMV-transfected cells was calculated for RhoA- and RhoC-transfected cells. For an MTS [3,4-(5-dimethylthiazol-2-yl)-5-(3-carboxymethoxy phenyl)-2-(4-sulfophenyl)-2H-tetrazolium salt]-based cytotoxicity study, Cos-7 cells were seeded at 3×10^4 cells per well of a 96-well plate and cotransfected with 0.2 μg of either RhoA, RhoC, or pCMV-script plasmid together with 0.02 μg of AAV2-luciferase plasmid. All wells were done in triplicate. After 24 h, CellTiter 96 AQueous One Solution Reagent was added to each well (1:10 dilution into medium), and the plate was incubated at 37°C for 2 h. Absorbance was read at 490 nm on a Molecular Devices SpectraMax M2 plate reader, and values were normalized against 5,000 RLU. The experiment was performed three times.

Statistical analysis. Statistical analysis was calculated using one-way analysis of variance (ANOVA), followed by a Bonferroni posttest or by an unpaired Student *t* test with GraphPad Prism 5 software.

RESULTS

RhoC expression correlates with EBOV and VSV pseudotyped vector transduction. To identify cellular proteins involved in EBOV pseudotyped vector transduction, we compared the gene expression profile in a panel of cell lines with their ability to be transduced by pseudovirions expressing either eGFP or β-galactosidase. Using COMPARE correlative analysis in combination with customized software to rank the strength of the correlation and to further clarify function, subcellular location, and signaling pathways of interest, we compared EBOV/FIV-β-galactosidase vector transduction profiles generated for each of 46 NCI cell lines with cDNA microarray databases that contain expression data on over 135,000 genes or expression patterns. A statistically significant correlation was observed between the pattern of EBOV/FIV-β-galactosidase transduction and the level of expression of RhoC, a member of the Rho GTPase family, in the microarray database. Statistical analysis calculated a PCC of 0.443 ($P < 0.002$). To better identify expression profiles that are associated with events mediated by the viral glycoprotein and not those mediated by the viral particle core and to determine if the correlation was specific for the EBOV envelope, COMPARE analysis was repeated using transduction data generated from EBOV/VSV-eGFP and VSV/VSV-eGFP as seed data. Again, a significant correlation was seen between the profile of EBOV GP pseudovirion transduction and RhoC expression, but a significant correlation was also observed with VSV/VSV-eGFP pseudovirion transduction and RhoC expression, with PCC values of 0.497 ($P < 0.001$) and 0.438 ($P < 0.001$), respectively. Therefore, using this bioinformatics approach, RhoC expression seems to be an important factor in both EBOV and VSV pseudotyped vector transduction, irrespective of the viral core used.

Correlation of Rho GTPase expression levels with transduction efficiency of EBOV and VSV pseudotyped vector in different cell lines. The Rho GTPases belong to the Ras superfamily of small GTP-binding proteins and are found in all eukaryotic cells. The best-characterized Rho GTPases are RhoA, which induces the formation of stress fibers (stiff actin bundles associated with myosin-based contractility that terminate in focal adhesions); Rac1, which induces lamellipodia (thin protrusive structures at the cell periphery); and Cdc42, which induces filopodia (finger-like projections) (2, 13). Although RhoB and RhoC were characterized at the same time as RhoA, they have received less attention because of their extensive homology to RhoA and because overexpression studies indicate similar functions (44). Small Rho GTPases have been found to play a role in internalization of many different viruses through their ability to regulate aspects of intracellular actin dynamics (12, 23, 24, 34, 43).

To confirm that transduction efficiency correlated with levels of Rho GTPase expression, we transduced four different cell lines, Cos-7, SNB-19, 293T, and Malme-3M with EBOV/MuLV and VSV/MuLV vectors expressing eGFP and compared our results to endogenous levels of RhoA, RhoB, and RhoC. EBOV/MuLV-eGFP had higher transduction activity, up to a 35-fold increase, on SNB-19 and Cos-7 cells than on 293T and Malme-3M cells ($P < 0.0001$) (Fig. 1A). VSV/MuLV-eGFP showed the same pattern of significantly greater overall transduction in SNB-19 and Cos-7 cells ($P < 0.001$ and $P < 0.0001$, respectively) (Fig. 1B), than in 293T and Malme-3M cells. Overall, EBOV/MuLV-eGFP transduced SNB-19 cells more efficiently than Cos-7 cells, and VSV/MuLV-eGFP transduced Cos-7 cells more efficiently than SNB-19 cells. Western blot analysis of Rho GTPases (approximately 20 kDa) in whole-cell lysate normalized to GAPDH expression showed that the concentration of endogenous RhoC correlated with increased transduction efficiency. The concentration of RhoC was greater in permissive cell lines SNB-19 and Cos-7 than in the weakly permissive cell lines, 293T and Malme-3M (Fig. 1C). In contrast, overall endogenous RhoA expression did not correlate with EBOV/MuLV-eGFP or VSV/MuLV-eGFP transduction. RhoA was present at a high concentration in Malme-3M cells even though these cells are weakly permissive to both MuLV vectors. The presence of endogenous RhoB was not detected in any of the cell lines. This correlates with gene expression data derived from the NCI panel of cells, where minimal RhoB RNA is made in SNB-19 and Malme-3M cells. Lysate from 293T cells overexpressing RhoC, RhoA, and RhoB proteins as a result of transfection with the relevant plasmids was included as a positive control for detection of the Rho proteins with corresponding antibodies (Fig. 1C, lane 1 versus lane 2). Relative band intensity for RhoC and RhoA was normalized to GAPDH, and the differences in expression levels between cell lines (Fig. 1D and E) correlated well with the difference observed with the microarray data for SNB-19 and Malme-3M cells (data not shown).

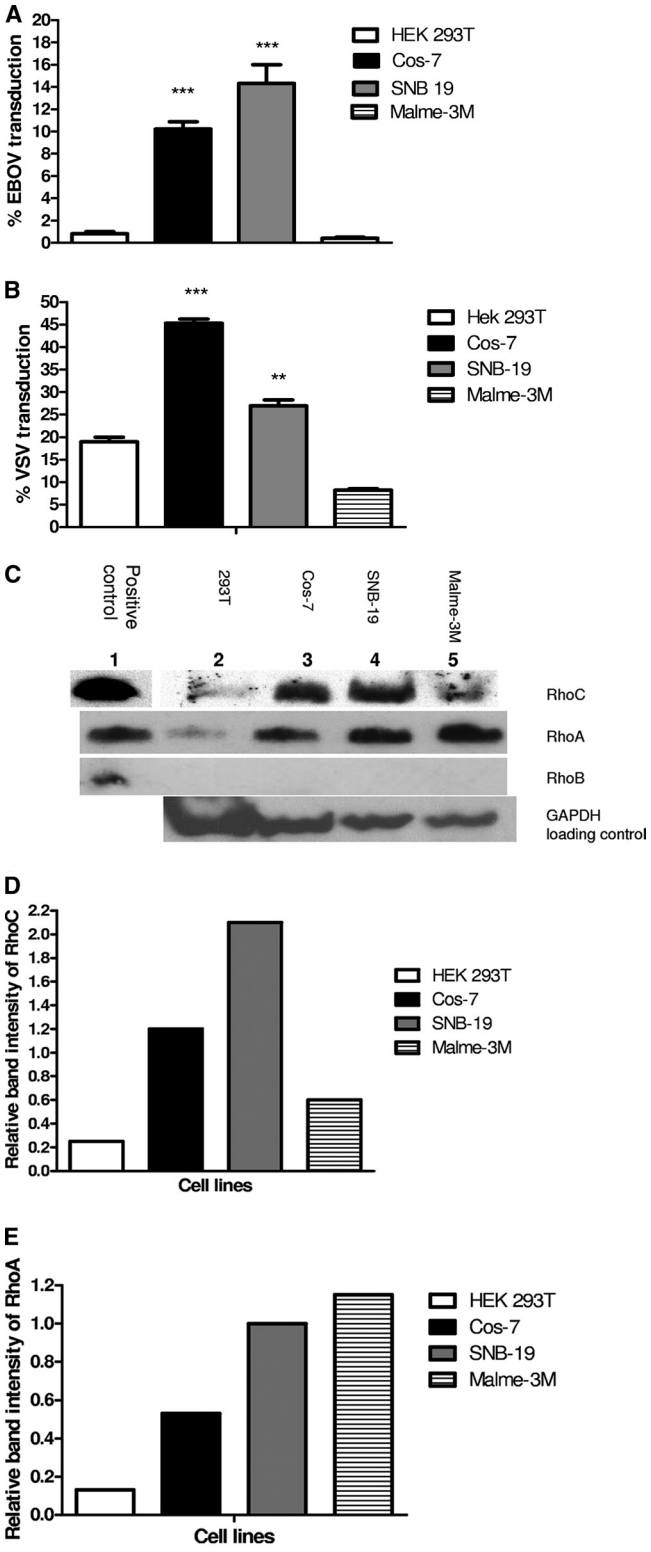

FIG. 1. Correlation of EBOV/MuLV-eGFP and VSV/MuLV-eGFP transduction efficiency with Rho GTPase expression in different cell lines. HEK 293T, Cos-7, SNB-19 and Malme-3M cells were transduced with either EBOV/MuLV-eGFP (A) or VSV/MuLV-eGFP (B) vectors at an MOI 1.5 for 60 h. Transduction efficiency was determined by measuring the percentage of eGFP-positive cells by FACS analysis. Error bars represent the standard error of the mean of three experiments done in triplicate. Statistical analysis was performed by one-way ANOVA to show the difference in transduction efficiency of Cos-7 and SNB-19 cells compared to 293T and Malme-3M cells. Bonferroni posttests were performed (**, $P < 0.001$; ***, $P < 0.0001$). (C) Western blot analysis was performed for detection of RhoC, RhoA, and RhoB in either transfected 293T cell lysate overexpressing the Rho proteins (lane 1) or in untransfected cell lysates from 293T, Cos-7, SNB-19, and Malme-3M cells grown under identical conditions. GAPDH detection was used as a loading control. The band intensities of endogenous RhoC (D) and Rho A (E) relative to the GAPDH control were quantified using Adobe Photoshop CS2 software.

Overexpression of RhoB and RhoC enhances EBOV and VSV pseudotyped vector transduction but not HIV pseudotyped or AAV2 vector transduction in 293T cells. To examine the effect of overexpression of Rho GTPases on MuLV pseudotyped transduction, weakly permissive 293T cells, transfected with either RhoA, RhoB, or RhoC plasmid, were transduced with EBOV/MuLV-eGFP and VSV/MuLV-eGFP vectors, and the transduction activity was compared with cells transfected with an empty plasmid, pCMV-script. Figure 1C can be referred to for evidence of overexpression of RhoC, RhoA, and RhoB proteins in 293T cells as a result of transfection with the relevant plasmids (lane 1 versus lane 2). To normalize transfection efficiency, a luciferase-encoding plasmid was included (1/10 dilution) in the transfection reaction mixture, and the number of eGFP-positive cells for each sample was normalized to the level of luciferase expression. RhoC-expressing cells significantly increased normalized EBOV/MuLV-eGFP and VSV/MuLV-eGFP transduction (percentage of GFP per 500,000 RLU) 8- and 12-fold, respectively, compared to pCMV-transfected control cells ($P < 0.05$) (Fig. 2A). RhoA-transfected cells showed only a slight increase in normalized transduction activity, whereas RhoB-transfected cells showed 11-fold and 25-fold increases in normalized EBOV/MuLV-eGFP and VSV/MuLV-eGFP transductions, respectively, ($P < 0.001$). These results confirm our bioinformatics correlation between RhoC expression and EBOV or VSV pseudotyped vector transduction and suggest that RhoB and RhoC play an important role in enhancing their transduction.

EBOV and VSV pseudotyped virions are reported to enter cells via an endosomal pathway (11, 30, 40). To determine if RhoC would affect other pseudotyped virions that can enter by direct fusion, we examined the effect of overexpression of Rho GTPases on HIV/HIV-eGFP vector transduction. HIV GP envelope has been shown to mediate virus fusion at the plasma membrane (5). When transduction was examined in Rho GTPase-overexpressing cells, sevenfold and sixfold increases in EBOV/HIV-eGFP transduction were seen in RhoB- and RhoC-expressing cells over pCMV-transfected control cells, respectively ($P < 0.001$ and $P < 0.05$, respectively) (Fig. 2B). RhoA-expressing cells showed minimal increase in transduction over pCMV control cells. In contrast to EBOV/HIV-eGFP data, overexpression of RhoB and RhoC had a minimal effect on HIV/HIV-eGFP transduction. Although both RhoB- and RhoC-expressing cells showed approximately a twofold increase in transduction, this difference was still significantly less than the increase seen in EBOV/HIV-eGFP transduction

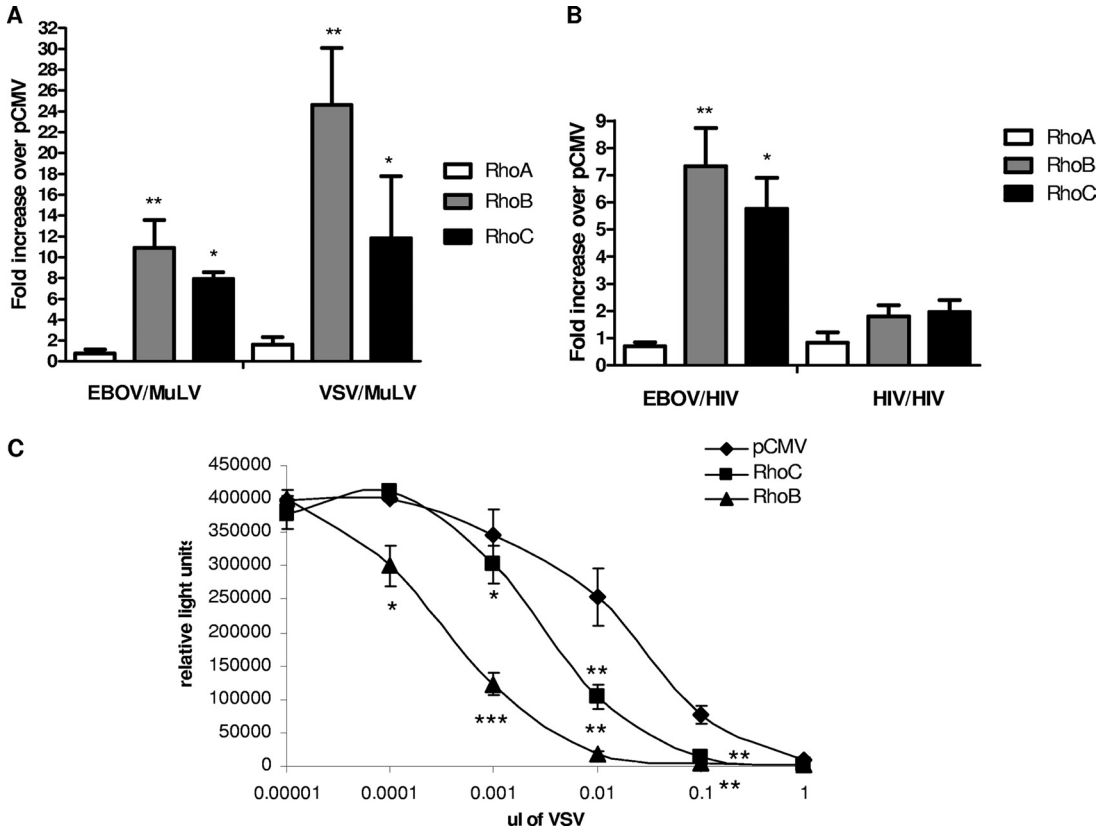

FIG. 2. Effect of Rho GTPase overexpression on EBOV, VSV, and HIV pseudotyped vector transduction and on VSV infection. HEK 293T cells were transiently cotransfected with either RhoA, RhoB, RhoC, or pCMV-script plasmid together with a plasmid expressing luciferase for 24 h and then transduced with different pseudotyped MuLV-eGFP or HIV-eGFP vectors (MOI of 1.5). Transduction efficiency was expressed as the percentage of eGFP normalized against 500,000 RLU. The relative increase in normalized EBOV/MuLV-eGFP or VSV/MuLV-eGFP transduction efficiency (A) or EBOV/HIV-eGFP or HIV/HIV-eGFP transduction efficiency (B) over pCMV-script control was calculated for RhoA-, RhoB-, and RhoC-transfected cells. (C) To examine the effect on VSV infection, HEK 293T cells were transfected with either pCMV plasmid, RhoB plasmid, or RhoC plasmid. At 48 h following transfection, cells were infected with VSV (Indiana) at an MOI of 0.001. Virus produced in the transfected cells was collected at 18 h following infection, and titers were determined by serial dilution of virus stocks on Vero cells. Relative cell numbers of adherent cells within the wells were assessed in an ATP Lite assay. Error bars represent the standard error of the mean of three experiments done in triplicate. Statistical comparison was performed by one-way ANOVA and Bonferroni posttest using GraphPad Prism 5 (*, $P < 0.05$; **, $P < 0.001$; ***, $P = 0.0001$) and by a paired student t test.

on transfection with RhoB and RhoC ($P < 0.05$). Again, RhoA had a minimal effect on HIV/HIV-eGFP transduction, indicating that it has no significant involvement in either EBOV, VSV, or HIV vector transduction.

The effect of Rho GTPase overexpression on transduction of a nonenveloped vector was also examined. AAV2 is a nonenveloped virus which predominantly enters cells by clathrin-mediated endocytosis subsequent to receptor binding (10). Overexpression of RhoA, RhoB, or RhoC produced no significant increase in AAV2 transduction efficiency compared with pCMV-transfected cells (data not shown).

Overexpression of RhoB and RhoC enhances VSV infection. Our findings with pseudovirions suggested that RhoB or RhoC expression would enhance entry of infectious VSV or EBOV, leading to production of higher titers. To examine if overexpression of RhoB or RhoC in 293T cells does indeed enhance VSV infection, we incubated RhoB- or RhoC-transfected cells with infectious VSV and collected supernatants at 18 h when signs of VSV replication were evident. Viral titers in the supernatants were evaluated by serially diluting the supernatants onto Vero cells. Infection of VSV in the Vero cells was assessed both by visual inspection of cell monolayers for VSV plaques (data not shown) and by the viability of the adherent monolayer at 36 h following infection since VSV infection causes detachment and killing of these target cells (Fig. 2C). Similar results were found with both assays. We found that the quantity of VSV generated in RhoC-expressing cells was significantly increased by about 10-fold over cells transfected with the empty vector. Expression of RhoB resulted in about 100-fold higher titers of VSV. These findings indicate that expression of RhoB or RhoC enhances the VSV production and is consistent with our transduction results with vectors.

***C. difficile* toxin B inhibits EBOV/MuLV-eGFP transduction in Rho GTPase-overexpressing cells.** In order to confirm our bioinformatics and overexpression data, 293T cells overexpressing RhoA, RhoB, or RhoC together with luciferase were treated with *C. difficile* toxin B, a potent inhibitor of Rho GTPases, prior to transduction with EBOV/MuLV-eGFP. The inhibitory effects of *C. difficile* toxin B, a monoglucosyltransferase that utilizes UDP-glucose, on Rho GTPases have been

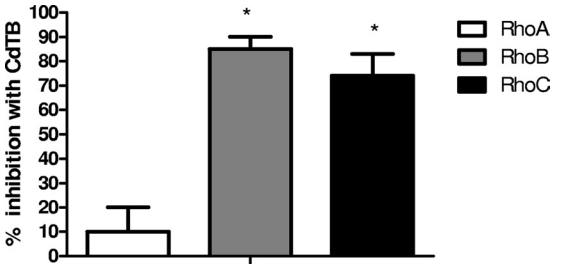

FIG. 3. Effect of the Rho GTPase inhibitor *C. difficile* toxin B on EBOV/MuLV-eGFP transduction. HEK 293T cells were transiently cotransfected with either RhoA, RhoB, RhoC, or pCMV-script plasmid together with a plasmid expressing luciferase; cells were treated with *C. difficile* toxin B (CdTB; 600 ng/well), a Rho GTPase activity inhibitor, and transduced with EBOV/MuLV-eGFP (MOI of 1.5). The percent transduction inhibition (normalized to 500,000 RLU) compared to untreated, transfected controls was calculated for *C. difficile* toxin B-treated, Rho-transfected cells. Error bars represent the standard error of the mean of three experiments done in triplicate. Statistical comparison was performed by one-way ANOVA and Bonferroni posttest using GraphPad Prism 5 (*, $P < 0.05$).

well documented (1, 17, 18, 32). Specifically, the toxin transfers its glucose moiety onto the Rho GTPase at a critical threonine residue located in the switch I region, inhibiting ADP-ribosylation of Rho. This glucosylation prevents Rho GTPases from associating with their effectors and consequently blocks the downstream signal transduction pathways leading to disaggregation of the actin filament. Substrate specificity of toxin B is restricted to the Rho subfamily GTPases, and all members of this subfamily such as Rho, Rac, and Cdc42 are glucosylated.

Treatment with *C. difficile* toxin B inhibited the increased transduction activity observed following transfection with RhoB and RhoC (Fig. 3). *C. difficile* toxin B-treated RhoB- and RhoC-overexpressing cells exhibited 85% and 75% inhibition, respectively, compared with untreated controls. Minimal inhibition in transduction was seen in *C. difficile* toxin B-treated RhoA-transfected cells (10%), and this was significantly less than in *C. difficile* toxin B-treated RhoB- and RhoC-transfected cells ($P < 0.05$). *C. difficile* toxin B-treated pCMV control-transfected cells showed no inhibition compared to an untreated control. Therefore, in agreement with our bioinformatics correlation and transient overexpression assay, inhibition of Rho GTPase activity reduced EBOV/MuLV-eGFP transduction efficiency in RhoB and RhoC GTPase-overexpressing cells.

RhoC-expressing cells allow greater fusion with EBOV VLPs. The Ras superfamily of small GTP-binding proteins has been reported to affect cell signal transduction, proliferation, vesicle trafficking, and regulation of the actin cytoskeleton (2, 13). Thus, their effect on pseudotyped MuLV transduction could be related to the trafficking of the core particle following internalization or on the internalization of viruses. In our initial bioinformatics-based studies of EBOV and VSV pseudotyped vector transduction, we used vectors containing two unrelated cores, FIV and VSV, and observed that a correlation between RhoC expression and transduction was core independent. Similarly, our RhoC overexpression data indicate that increased vector transduction is dependent on pseudotyping with EBOV GP whereby increased RhoC expression results in enhanced EBOV/HIV but not HIV/HIV transduction. These findings suggest that the role of RhoC may be related more to entry than to core trafficking. To determine if RhoC is involved in viral glycoprotein-mediated internalization rather than intracellular trafficking of viral core DNA, we examined the effect of RhoA and RhoC on internalization of EBOV VLPs (Fig. 4). 293T cells overexpressing RhoA or RhoC were incubated with EBOV VLPs tagged with Src-β-lactamase and loaded with the fluorescent substrate CCF2/AM. Following internalization into endosomes, the labeled VLPs fuse with the endosomal membrane and are released into the cytoplasm, where the cephalosporin ring of the CCF2/AM is hydrolyzed by the β-lactamase, causing a shift in the emission spectrum from 520 nm (green) to 447 nm (blue) after excitation of the cell. Fusion and entry into the cytoplasm were visualized and scored by fluorescence microscopy. Cells were incubated with EBOV GP-deficient VLPs as a negative control. These cells showed no blue cells when loaded with CCF2/AM substrate (Fig. 4A). pCMV- and RhoA-transfected cells showed few, faintly blue cells after incubation with EBOV VLPs and loading with CCF2/AM substrate (Fig. 4B and C). In comparison, RhoC-transfected cells showed many blue cells which were clearly visible in different fields (Fig. 4D). Figure 1C can be referred to for evidence of overexpression of RhoA and RhoC proteins in 293T cells as a result of transfection with the relevant plasmids (Fig. 1C, lane 1 versus lane 2). Quantification of the relative increase in blue fluorescence over the pCMV control indicated an approximately 2.75-fold increase in EBOV VLP entry of RhoC-transfected cells compared with an approximately 1.5-fold increase in RhoA-transfected cells ($P < 0.01$) (Fig. 4E). This finding suggests that the effect of RhoC on EBOV particle transduction is greater than that of RhoA, is likely at the entry phase, and is related to the envelope.

RhoC-expressing cells allow greater internalization of Alexa Fluor 488-dextran conjugate by nonspecific endocytosis. While the above data suggest that RhoC can affect the entry phase of vector transduction, because of its effect on two very diverse viruses, it is likely that this occurs by a nonspecific uptake mechanism rather than a specific interaction between RhoC and the virus. Furthermore, Western blotting of fractionated cell extract from cells transfected with RhoC suggests that the vast majority of RhoC was in the cytoplasm and not associated with the plasma membrane (data not shown). To examine the ability of RhoA- and RhoC-overexpressing cells to internalize exogenous material by nonspecific endocytosis, uptake of Alexa Fluor 488-dextran conjugate was measured. RhoC-expressing cells showed a fourfold increase in internalized fluorescent conjugate over pCMV-expressing control cells (data not shown). 293T cells transiently expressing RhoA showed a minimal increase in dextran uptake over pCMV and was significantly less than with RhoC ($P < 0.01$). In agreement with the VLP data, this indicates an increase in vector internalization as a result of RhoC expression. This finding indicates that RhoC-expressing cells have a greater ability than RhoA-expressing cells to take up exogenous material by nonspecific endocytosis, suggesting that elevated expression of RhoC in 293T cells enhances fluid-phase endocytosis.

RhoC expression induces an extensive actin stress fiber network. Rho GTPases have been reported to regulate remodeling of the actin cytoskeleton during cell morphogenesis and

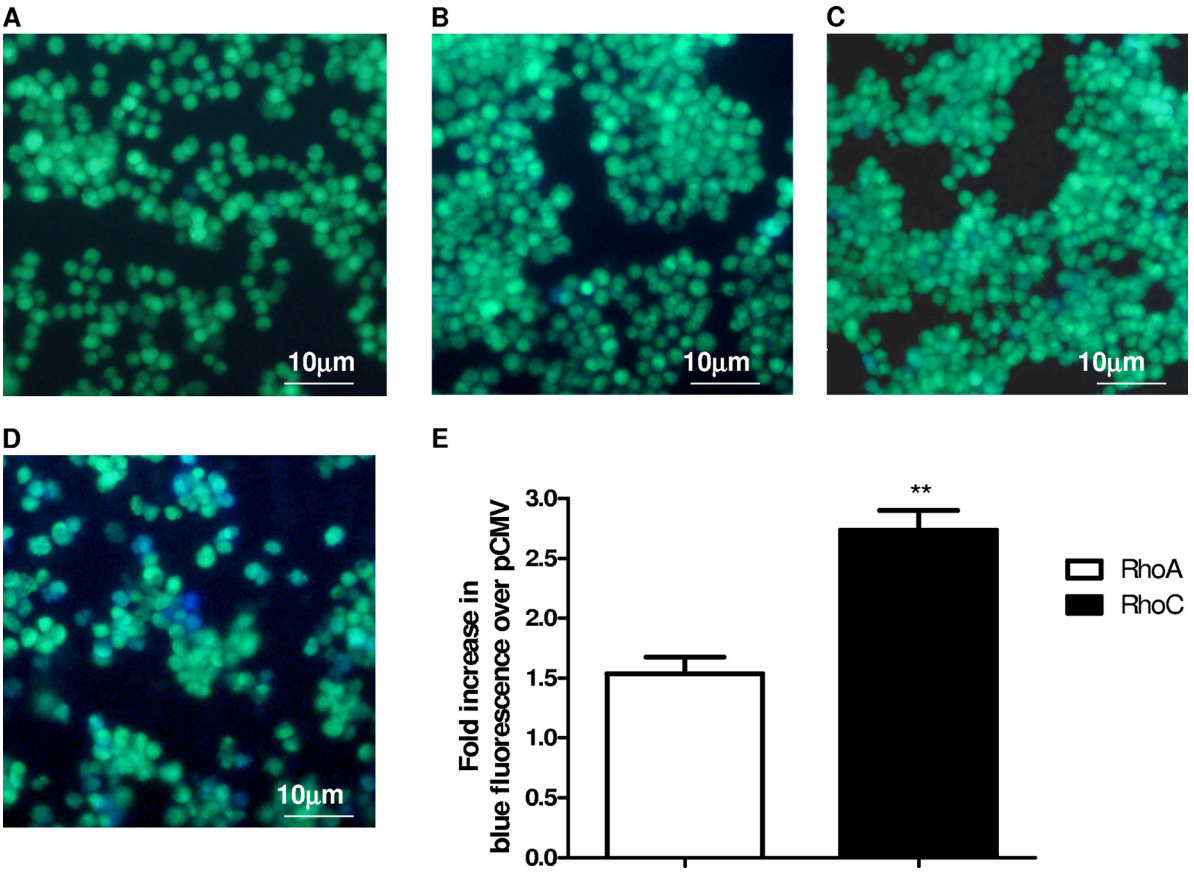

FIG. 4. Effect of Rho GTPases on EBOV VLP fusion. HEK 293T cells were transfected with either pCMV-script (B), RhoA (C), or RhoC (D) plasmids and incubated with Src-β-lactamase-labeled EBOV VLPs for 12 h. Untransfected cells were incubated with EBOV GP-deficient VLPs as a negative control (A). β-Lactamase substrate, CCF2/AM, was added to allow visualization of VLP fusion, causing a shift in fluorescence from green (530 nm) to blue (447 nm). Images were captured by fluorescent microscopy using a β-lactamase filter. All images were viewed with a 20× objective. Scales are indicated on each image. (E) Blue fluorescence per square pixel was calculated for five images using NIH ImageJ software. Background fluorescence of untransfected, untreated cells was subtracted from values. The mean relative increase in blue fluorescence of RhoA- and RhoC-transfected cells over pCMV control cells was calculated. Error bars represent the standard error of the relative increase in fluorescence. Statistical comparison was performed by an unpaired Student *t* test using GraphPad Prism 5 (**, $P < 0.01$).

motility, and its activation can create membrane ruffling, stimulating bulk pinocytosis (2, 13). A key event in creating the membrane ruffles is the formation of actin stress fibers in the cell. Our earlier findings on increased internalization would suggest that RhoC has a greater effect on stress actin fiber formation than RhoA. To compare stress fiber formation, RhoA- or RhoC-transfected cells were fixed and stained with Alexa Fluor 546-labeled phalloidin, and the stress fibers were visualized and quantified by fluorescence confocal microscopy (Fig. 5). RhoA-transfected cells (Fig. 5C) did show increased intensity of actin polarization or development of stress fibers compared to untransfected control cells (Fig. 5A), but this was not obvious compared with pCMV control-transfected cells (Fig. 5B). In contrast, RhoC-transfected cells (Fig. 5D) showed more intense staining of the F-actin due to the formation of stress fibers. RhoC-transfected cells showed a significantly greater relative increase, approximately 12-fold, in fluorescence intensity over the pCMV control than RhoA-transfected cells ($P < 0.001$) (Fig. 5E). This finding suggests that RhoC promotes reorganization of the actin filament into stress fibers to a greater extent than RhoA and supports the role of RhoC in pseudotyped EBOV and VSV transduction by increasing nonspecific uptake, likely by macropinocytosis. We eliminated the possibility that the increased formation of actin stress fibers in RhoC-transfected cells was due to increased cytotoxic effect in these cells compared to RhoA- and pCMV-transfected cells by measuring the viability of Cos-7 cells 24 h posttransfection with RhoA, RhoC, and pCMV plasmids using an MTS-based cytotoxicity assay. No significant difference was seen between the absorbance of RhoC-transfected cells and the other transfected groups when values were normalized per 5,000 RLU (data not shown).

DISCUSSION

The viral GP/receptor interactions of EBOV and VSV are poorly understood, but both viruses have a broad but defined cell tropism (7, 25, 41, 45). As a first step in cell infection, entry by macropinocytosis is an attractive pathway and could be used by a wide variety of viruses. Macropinosomes can become acidified and can intersect with endocytic vesicles (14). Low-pH events are known to trigger conformational changes

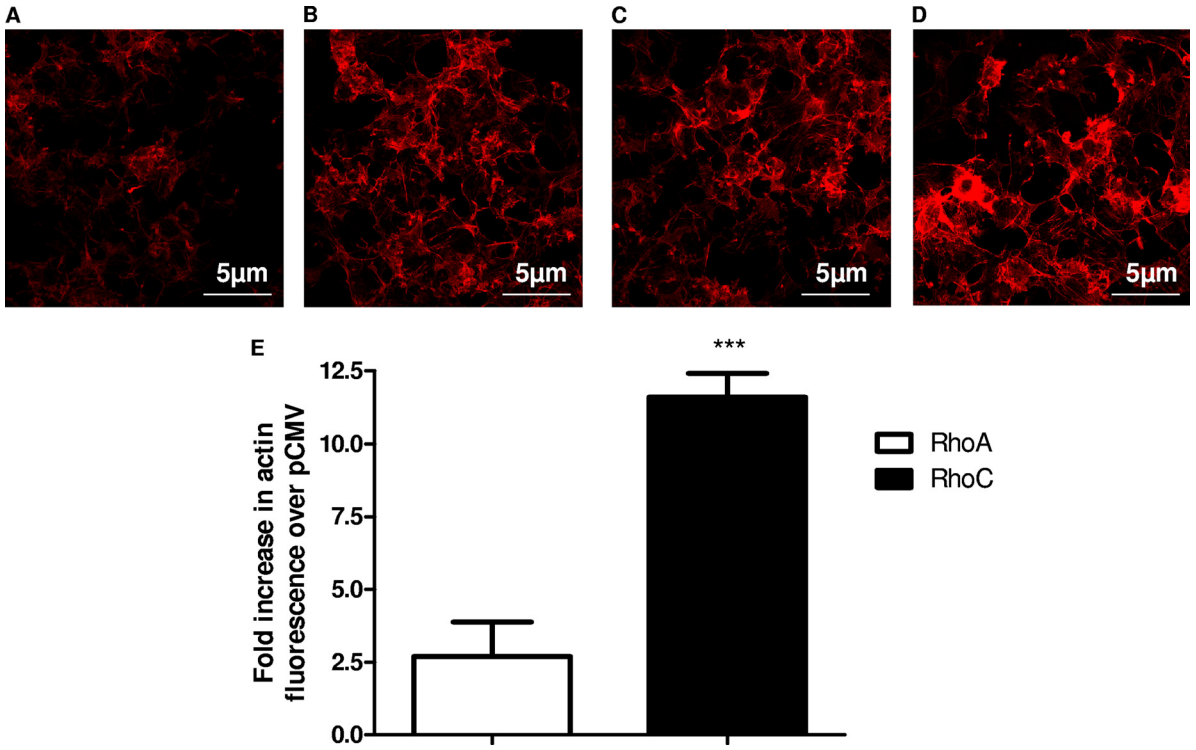

FIG. 5. Effect of Rho GTPases on the actin filament organization. Cos-7 cells were transiently cotransfected with either RhoA, RhoC, or pCMV-script together with a nuclear GFP-expressing plasmid and stained with Alexa Fluor 546-conjugated phalloidin after 24 h. Untransfected, phalloidin-stained cells were included as a control (A); pCMV (B)-, RhoA (C)-, and RhoC (D)-positive cells were identified by positive nuclear GFP staining, and images of phalloidin staining were captured using an oil objective (63×) by confocal fluorescent microscopy. (E) Actin fluorescence intensity of eight cells was quantified for RhoA-, RhoC-, and pCMV-transfected, phalloidin-stained cells using NIH ImageJ software. Background phalloidin staining of untransfected cells was subtracted from overall values. The mean relative increase in phalloidin staining over the GFP/pCMV control was calculated for GFP/RhoA or GFP/RhoC images. Error bars represent the standard error of the mean relative increase in fluorescence. Statistical comparison was performed by unpaired Student *t* test in GraphPad Prism 5 (***, $P < 0.001$).

in the viral particle and convert the particle into an active state that can bind a receptor protein and enter the cytoplasm. In this study we present initial evidence that EBOV and VSV uptake into endosomes is enhanced by RhoB or RhoC, with the possibility that this is due to macropinocytosis.

While previous research has indicated the role of actin polymerization in virion transduction (34, 43), our finding of a specific role for RhoB and RhoC in pseudotyped vector entry is unique. Furthermore, VSV and EBOV represent two very distinct families of viruses and likely use different host factors for attachment, yet they converge on a common Rho-mediated pathway, suggesting that this may be a route of entry utilized by many different viruses. Through the use of comparative gene analysis, we found a strong correlation between permissivity of cell lines to EBOV GP and VSVG pseudotyped transduction and RhoC expression, indicating that RhoC could play a role in uptake of virions pseudotyped with unrelated viral glycoproteins. To date, RhoC has not been specifically implicated in virion uptake, but other Rho GTPases, Rac1, RhoA, and Cdc42, are well established as mediators in the nonspecific endocytosis of many enveloped viruses such as vaccinia virus, herpesvirus, and paramyxovirus (12, 24, 34). Through their ability to alternate between an active GTP-bound form and an inactive GDP-bound form, these Rho GTPases cause actin phosphorylation that activates different downstream effector molecules. These effector molecules initiate signal transduction pathways and result in subsequent rearrangements in the actin cytoskeleton that are required for blebbing events associated with fluid-phase endocytosis such as macropinocytosis (2). Some previous studies have implicated the actin cytoskeleton in EBOV entry, where agents such as cytochalasin D and swinholide A that impair microfilament function inhibited GP-mediated entry (47). Though it has been well established that VSV enters mostly by clathrin-coated endocytosis (40), some studies do indicate the involvement of macropinocytosis as an alternative pathway in VSV uptake (4). The use of electron microscopy showed a significant concentration of VSV particles in large, noncoated macropinosome-like vesicles similar to cytoplasmic inlets and phagocytic vacuoles 1 h after VSV adsorption at 37°C. Similarly, VSV pseudovirions have been shown to undergo actin- and myosin-driven movement along filopodia prior to cell entry, where addition of cytochalasin D and blebbistatin, a specific inhibitor of myosin II, inhibited further movement and infection of filopodia and microvilli-rich cells (22).

When the effects of RhoA, RhoB, and RhoC overexpression on the transduction of enveloped HIV GP pseudotyped HIV virions, which enter by membrane fusion (5, 46), and nonenveloped AAV2, which undergoes endocytosis (10), were examined, none of the Rho proteins had any significant effect on

uptake of either type of viral particle. This strengthens the argument that RhoB and RhoC involvement is specific for a subset of virions such as those pseudotyped with EBOV or VSV glycoprotein and does not play a role in nonspecific uptake of all enveloped viruses and nonenveloped viruses which enter by endocytosis.

No definitive correlation was seen between permissivity to EBOV/MuLV or VSV/MuLV and RhoA expression, and no detectable RhoB was found in any of the cell lines. RhoB expression is more highly regulated than that of RhoA and RhoC; therefore, its absence may be due to its substantially shorter half-life of 30 min (27, 49). Although RhoB appears to affect virion uptake in a manner similar to RhoC when it is overexpressed, it is not expressed at sufficiently high levels in the NCI60 cells to detect, indicating that its endogenous expression is not important for EBOV GP-dependent uptake.

RhoC was not the only gene whose expression strongly correlated with EBOV GP transduction. For example, β-actin also had a high PCC value. While a role for β-actin in EBOV GP-dependent entry has not yet been demonstrated, studies with retroviruses indicate that actin polymerization is necessary for cellular receptor/coreceptor recruitment, membrane fusion events, endocytosis of viral particles, and generation of a functional RT complex. Another group of proteins that were positively correlated in this analysis were cell adhesion molecules, such as integrins αVI and αIII and gap junction protein α1. This correlation is intriguing since expression of a full-length EBOV GP containing the mucin domain results in down-modulation of integrin αVβ3 from the surface of infected cells. This down-modulation of surface proteins is reminiscent of retroviral envelope down-modulation of cellular receptors on the surface of infected cells. Further study will be required to understand these gene changes in the context of the effect of RhoC on EBOV transduction.

Although pseudotyped vectors allow us some means of looking at the tropism that a viral GP has for certain cell types, the pseudovirions contain an unrelated viral core, which raises some concerns in differentiating between internalization and intracellular trafficking mediated by transduction of the viral DNA. VLPs labeled with β-lactamase lack a viral genome, and their cores are composed solely of EBOV matrix protein VP40; therefore, they allow us to look specifically at internalization. Overexpression of RhoC led to greater fusion of the EBOV VLPs than with the pCMV control and RhoA as well as to a significant increase in stress fibers and uptake of fluorescent dextran compared with the pCMV control and RhoA, indicating that RhoC's involvement in vector entry likely occurs early in the transduction pathway prior to late endosomal escape, viral replication, and assembly.

ACKNOWLEDGMENTS

We thank William Swaim for help with confocal microscopy and Thomas Bugge for use of his fluorescent microscope for EBOV VLP imaging. We thank Melissa Hickey for assistance with lentiviral vector production.

This work was supported by an Intramural NIAID biofense grant to J. A. Chiorini and an NIAID grant (064526) to Wendy Maury.

REFERENCES

1. **Ando, Y., S. Yasuda, F. Oceguera-Yanez, and S. Narumiya.** 2007. Inactivation of Rho GTPases with *Clostridium difficile* toxin B impairs centrosomal activation of Aurora-A in G_2/M transition of HeLa cells. Mol. Biol. Cell **18:**3752–3763.
2. **Bishop, A. L., and A. Hall.** 2000. Rho GTPases and their effector proteins. Biochem. J. **348:**241–255.
3. **Brindley, M. A., L. Hughes, A. Ruiz, P. B. McCray, Jr., A. Sanchez, D. A. Sanders, and W. Maury.** 2007. Ebola virus glycoprotein 1: identification of residues important for binding and postbinding events. J. Virol. **81:**7702–7709.
4. **Cernescu, C., S. N. Constantinescu, and L. M. Popescu.** 1990. Electron microscopic observations of vesicular stomatitis virus particles penetration in human fibroblasts. Rev. Roum. Virol. **41:**93–96.
5. **Chan, D. C., and P. S. Kim.** 1998. HIV entry and its inhibition. Cell **93:**681–684.
6. **Chan, S. Y., C. J. Empig, F. J. Welte, R. F. Speck, A. Schmaljohn, J. F. Kreisberg, and M. A. Goldsmith.** 2001. Folate receptor-alpha is a cofactor for cellular entry by Marburg and Ebola viruses. Cell **106:**117–126.
7. **Chan, S. Y., R. F. Speck, M. C. Ma, and M. A. Goldsmith.** 2000. Distinct mechanisms of entry by envelope glycoproteins of Marburg and Ebola (Zaire) viruses. J. Virol. **74:**4933–4937.
8. **Chandran, K., N. J. Sullivan, U. Felbor, S. P. Whelan, and J. M. Cunningham.** 2005. Endosomal proteolysis of the Ebola virus glycoprotein is necessary for infection. Science **308:**1643–1645.
9. **Coil, D. A., and A. D. Miller.** 2004. Phosphatidylserine is not the cell surface receptor for vesicular stomatitis virus. J. Virol. **78:**10920–10926.
10. **Duan, D., Q. Li, A. W. Kao, Y. Yue, J. E. Pessin, and J. F. Engelhardt.** 1999. Dynamin is required for recombinant adeno-associated virus type 2 infection. J. Virol. **73:**10371–10376.
11. **Empig, C. J., and M. A. Goldsmith.** 2002. Association of the caveola vesicular system with cellular entry by filoviruses. J. Virol. **76:**5266–5270.
12. **Favoreel, H. W., L. W. Enquist, and B. Feierbach.** 2007. Actin and Rho GTPases in herpesvirus biology. Trends Microbiol. **15:**426–433.
13. **Hall, A.** 2005. Rho GTPases and the control of cell behaviour. Biochem. Soc. Trans. **33:**891–895.
14. **Hewlett, L. J., A. R. Prescott, and C. Watts.** 1994. The coated pit and macropinocytic pathways serve distinct endosome populations. J. Cell Biol. **124:**689–703.
15. **Johnson, R. F., P. Bell, and R. N. Harty.** 2006. Effect of Ebola virus proteins GP, NP and VP35 on VP40 VLP morphology. Virol. J. **3:**31.
16. **Johnston, J. C., M. Gasmi, L. E. Lim, J. H. Elder, J. K. Yee, D. J. Jolly, K. P. Campbell, B. L. Davidson, and S. L. Sauter.** 1999. Minimum requirements for efficient transduction of dividing and nondividing cells by feline immunodeficiency virus vectors. J. Virol. **73:**4991–5000.
17. **Just, I., G. Fritz, K. Aktories, M. Giry, M. R. Popoff, P. Boquet, S. Hegenbarth, and C. von Eichel-Streiber.** 1994. *Clostridium difficile* toxin B acts on the GTP-binding protein Rho. J. Biol. Chem. **269:**10706–10712.
18. **Just, I., J. Selzer, M. Wilm, C. von Eichel-Streiber, M. Mann, and K. Aktories.** 1995. Glucosylation of Rho proteins by *Clostridium difficile* toxin B. Nature **375:**500–503.
19. **Kaletsky, R. L., G. Simmons, and P. Bates.** 2007. Proteolysis of the Ebola virus glycoproteins enhances virus binding and infectivity. J. Virol. **81:**13378–13384.
20. **Koo, H. M., A. Monks, A. Mikheev, L. V. Rubinstein, M. Gray-Goodrich, M. J. McWilliams, W. G. Alvord, H. K. Oie, A. F. Gazdar, K. D. Paull, H. Zarbl, and G. F. Vande Woude.** 1996. Enhanced sensitivity to 1-beta-D-arabinofuranosylcytosine and topoisomerase II inhibitors in tumor cell lines harboring activated *ras* oncogenes. Cancer Res. **56:**5211–5216.
21. **Lakadamyali, M., M. J. Rust, and X. Zhuang.** 2004. Endocytosis of influenza viruses. Microbes Infect. **6:**929–936.
22. **Lehmann, M. J., N. M. Sherer, C. B. Marks, M. Pypaert, and W. Mothes.** 2005. Actin- and myosin-driven movement of viruses along filopodia precedes their entry into cells. J. Cell Biol. **170:**317–325.
23. **Li, E., D. Stupack, G. M. Bokoch, and G. R. Nemerow.** 1998. Adenovirus endocytosis requires actin cytoskeleton reorganization mediated by Rho family GTPases. J. Virol. **72:**8806–8812.
24. **Locker, J. K., A. Kuehn, S. Schleich, G. Rutter, H. Hohenberg, R. Wepf, and G. Griffiths.** 2000. Entry of the two infectious forms of vaccinia virus at the plasma membrane is signaling-dependent for the IMV but not the EEV. Mol. Biol. Cell **11:**2497–2511.
25. **Marsh, M., and A. Helenius.** 1989. Virus entry into animal cells. Adv. Virus Res. **36:**107–151.
26. **Marzi, A., A. Akhavan, G. Simmons, T. Gramberg, H. Hofmann, P. Bates, V. R. Lingappa, and S. Pohlmann.** 2006. The signal peptide of the ebolavirus glycoprotein influences interaction with the cellular lectins DC-SIGN and DC-SIGNR. J. Virol. **80:**6305–6317.
27. **Prendergast, G. C.** 2001. Farnesyltransferase inhibitors define a role for RhoB in controlling neoplastic pathophysiology. Histol. Histopathol. **16:**269–275.
28. **Reed-Inderbitzin, E., and W. Maury.** 2003. Cellular specificity of HIV-1 replication can be controlled by LTR sequences. Virology **314:**680–695.
29. **Rodriguez, L. L.** 2002. Emergence and re-emergence of vesicular stomatitis in the United States. Virus Res. **85:**211–219.
30. **Sanchez, A.** 2007. Analysis of filovirus entry into vero e6 cells, using inhib-

itors of endocytosis, endosomal acidification, structural integrity, and cathepsin (B and L) activity. J. Infect. Dis. **196**(Suppl. 2)**:**S251–S258.
31. **Schlegel, R., T. S. Tralka, M. C. Willingham, and I. Pastan.** 1983. Inhibition of VSV binding and infectivity by phosphatidylserine: is phosphatidylserine a VSV-binding site? Cell **32:**639–646.
32. **Schmidt, M., U. Rumenapp, C. Bienek, J. Keller, C. von Eichel-Streiber, and K. H. Jakobs.** 1996. Inhibition of receptor signaling to phospholipase D by *Clostridium difficile* toxin B. Role of Rho proteins. J. Biol. Chem. **271:**2422–2426.
33. **Schornberg, K., S. Matsuyama, K. Kabsch, S. Delos, A. Bouton, and J. White.** 2006. Role of endosomal cathepsins in entry mediated by the Ebola virus glycoprotein. J. Virol. **80:**4174–4178.
34. **Schowalter, R. M., M. A. Wurth, H. C. Aguilar, B. Lee, C. L. Moncman, R. O. McCann, and R. E. Dutch.** 2006. Rho GTPase activity modulates paramyxovirus fusion protein-mediated cell-cell fusion. Virology **350:**323–334.
35. **Shimojima, M., Y. Ikeda, and Y. Kawaoka.** 2007. The mechanism of Axl-mediated Ebola virus infection. J. Infect. Dis. **196**(Suppl. 2)**:**S259–S263.
36. **Shimojima, M., A. Takada, H. Ebihara, G. Neumann, K. Fujioka, T. Irimura, S. Jones, H. Feldmann, and Y. Kawaoka.** 2006. Tyro3 family-mediated cell entry of Ebola and Marburg viruses. J. Virol. **80:**10109–10116.
37. **Sieczkarski, S. B., and G. R. Whittaker.** 2002. Dissecting virus entry via endocytosis. J. Gen. Virol. **83:**1535–1545.
38. **Sinn, P. L., M. A. Hickey, P. D. Staber, D. E. Dylla, S. A. Jeffers, B. L. Davidson, D. A. Sanders, and P. B. McCray, Jr.** 2003. Lentivirus vectors pseudotyped with filoviral envelope glycoproteins transduce airway epithelia from the apical surface independently of folate receptor alpha. J. Virol. **77:**5902–5910.
39. **Sullivan, N., Z. Y. Yang, and G. J. Nabel.** 2003. Ebola virus pathogenesis: implications for vaccines and therapies. J. Virol. **77:**9733–9737.
40. **Sun, X., V. K. Yau, B. J. Briggs, and G. R. Whittaker.** 2005. Role of clathrin-mediated endocytosis during vesicular stomatitis virus entry into host cells. Virology **338:**53–60.
41. **Superti, F., L. Seganti, F. M. Ruggeri, A. Tinari, G. Donelli, and N. Orsi.** 1987. Entry pathway of vesicular stomatitis virus into different host cells. J. Gen. Virol. **68:**387–399.
42. **Takada, A., C. Robison, H. Goto, A. Sanchez, K. G. Murti, M. A. Whitt, and Y. Kawaoka.** 1997. A system for functional analysis of Ebola virus glycoprotein. Proc. Natl. Acad. Sci. USA **94:**14764–14769.
43. **Veettil, M. V., N. Sharma-Walia, S. Sadagopan, H. Raghu, R. Sivakumar, P. P. Naranatt, and B. Chandran.** 2006. RhoA-GTPase facilitates entry of Kaposi's sarcoma-associated herpesvirus into adherent target cells in a Src-dependent manner. J. Virol. **80:**11432–11446.
44. **Wheeler, A. P., and A. J. Ridley.** 2004. Why three Rho proteins? RhoA, RhoB, RhoC, and cell motility. Exp. Cell Res. **301:**43–49.
45. **Wool-Lewis, R. J., and P. Bates.** 1998. Characterization of Ebola virus entry by using pseudotyped viruses: identification of receptor-deficient cell lines. J. Virol. **72:**3155–3160.
46. **Wyatt, R., and J. Sodroski.** 1998. The HIV-1 envelope glycoproteins: fusogens, antigens, and immunogens. Science **280:**1884–1888.
47. **Yonezawa, A., M. Cavrois, and W. C. Greene.** 2005. Studies of Ebola virus glycoprotein-mediated entry and fusion by using pseudotyped human immunodeficiency virus type 1 virions: involvement of cytoskeletal proteins and enhancement by tumor necrosis factor alpha. J. Virol. **79:**918–926.
48. **Zaharevitz, D. W., S. L. Holbeck, C. Bowerman, and P. A. Svetlik.** 2002. COMPARE: a web accessible tool for investigating mechanisms of cell growth inhibition. J. Mol. Graph. Model. **20:**297–303.
49. **Zalcman, G., V. Closson, G. Linares-Cruz, F. Lerebours, N. Honore, A. Tavitian, and B. Olofsson.** 1995. Regulation of Ras-related RhoB protein expression during the cell cycle. Oncogene **10:**1935–1945.